Title

STAT3 Activation as a Predictive Biomarker for Ruxolitinib Response in Head and Neck Cancer.

Journal

Clinical Cancer Research, 28(21)

ISSN

1078-0432

Authors

Qureshy, Zoya
Li, Hua
Zeng, Yan
et al.

Publication Date

2022-11-01

DOI

10.1158/1078-0432.ccr-22-0744

Peer reviewed

HHS Public Access

Author manuscript

Clin Cancer Res. Author manuscript; available in PMC 2023 November 01.

Published in final edited form as:

Clin Cancer Res. 2022 November 01; 28(21): 4737–4746. doi:10.1158/1078-0432.CCR-22-0744.

STAT3 activation as a predictive biomarker for ruxolitinib response in head and neck cancer

Zoya Qureshy[1,*], **Hua Li**[1,*], **Yan Zeng**[1], **Jose Rivera**[1], **Ning Cheng**[1], **Christopher N. Peterson**[1], **Mi-Ok Kim**[2,3], **William R. Ryan**[1], **Patrick K. Ha**[1], **Julie E. Bauman**[4], **Steven J. Wang**[5], **Steven R. Long**[6], **Daniel E. Johnson**[1], **Jennifer R. Grandis**[1]

[1]Department of Otolaryngology-Head and Neck Surgery, University of California San Francisco, San Francisco, California, 94143

[2]Department of Epidemiology and Biostatistics, University of California San Francisco, San Francisco, California, 94143

[3]Helen Diller Family Comprehensive Cancer Center, University of California San Francisco, San Francisco, California, 94143

[4]Division of Hematology and Oncology, University of Arizona College of Medicine, Tucson, Arizona, 85724

[5]Department of Otolaryngology-Head and Neck Surgery, University of Arizona College of Medicine, Tucson, Arizona, 85724

[6]Department of Pathology, University of California San Francisco, San Francisco, California, 94143

Abstract

Purpose: Increased activity of STAT3 is associated with progression of head and neck squamous cell carcinoma (HNSCC). Upstream activators of STAT3, such as JAKs, represent potential targets for therapy of solid tumors, including HNSCC. In this study we investigated the anti-cancer effects of ruxolitinib, a clinical JAK1/2 inhibitor, in HNSCC preclinical models including patient-derived xenografts (PDXs) from patients treated on a window-of-opportunity trial.

Methods: HNSCC cell lines were treated with ruxolitinib, and the impact on activated STAT3 levels, cell growth, and colony formation was assessed. PDXs were generated from HNSCC patients who received a brief course of neoadjuvant ruxolitinib on a clinical trial. The impact of ruxolitinib on tumor growth and STAT3 activation was assessed.

Results: Ruxolitinib inhibited STAT3 activation, cellular growth and colony formation of HNSCC cell lines. Ruxolitinib treatment of mice bearing a HNSCC cell line-derived xenograft significantly inhibited tumor growth compared with vehicle-treated controls. The response of HNSCC PDXs derived from patients on the clinical trial mirrored the responses seen in the neoadjuvant setting. Baseline active STAT3 (pSTAT3) and total STAT3 levels were lower, and ruxolitinib inhibited STAT3 activation in a PDX from a patient whose disease was stable on

Corresponding Authors: Jennifer R. Grandis.
*These authors contributed equally to the work

ruxolitinib, compared to a PDX from a patient whose disease progressed on ruxolitinib and where ruxolitinib treatment had minimal impact on STAT3 activation.

Conclusions: Ruxolitinib exhibits antitumor effects in HNSCC preclinical models. Baseline pSTAT3 or total STAT3 levels in the tumor may serve as predictive biomarkers to identify patients most likely to respond to ruxolitinib.

Keywords

head and neck squamous cell carcinoma (HNSCC); Janus kinase (JAK) inhibitor; patient-derived xenograft (PDX); ruxolitinib; signal transducer and activator of transcription 3 (STAT3)

Introduction

Signal transducer and activator of transcription 3 (STAT3), in its active, phosphorylated form, is a transcription factor regulating genes that mediate cell cycle progression, cellular proliferation and survival, and epithelial-to-mesenchymal transition (1). Overexpression and/or hyperactivation of this oncogene is common in head and neck squamous cell carcinoma (HNSCC) and other solid tumors and has been associated with progression and poor prognosis (2–5). Transcription factors, including STAT3, remain challenging therapeutic targets. Blockade of upstream receptor and non-receptor kinases, such as Janus kinases (JAKs), represents a feasible approach to abrogate STAT3 activation in tumors (3,6).

To date, three orally bioavailable JAK inhibitors have been FDA-approved: (1) the ATP-competitive JAK1/2 inhibitor ruxolitinib for myeloproliferative diseases and graft versus host disease, (2) the JAK2 inhibitor fedratinib for myeloproliferative diseases, and (7) the JAK3 inhibitor tofacitinib for rheumatoid arthritis and inflammatory bowel disease (8–11). In hematological malignancies such as polycythemia vera and myelofibrosis, an activating JAK2 V617F mutation drives hyperactivation of STAT3. Ruxolitinib and, more recently, fedratinib have been shown to decrease STAT3 activation and are viable treatment options for these conditions (12–17). However, the impact of JAK inhibition on solid tumor growth is incompletely understood.

Promising preclinical studies showed that JAK inhibition with the small molecule, ATP- competitive inhibitor AZD1480 decreased STAT3 activation in a variety of solid tumors (18). We previously reported that JAK inhibition by AZD1480 decreased STAT3 activation in HNSCC cell lines and suppressed tumor growth in PDXs (19). However, clinical trials of AZD1480 were discontinued due to neurotoxicity (20). Ruxolitinib, a well-tolerated JAK1/2 inhibitor, has also been explored in preclinical solid tumor models. Treatment with ruxolitinib decreased levels of phosphorylated STAT3 and inhibited cellular proliferation and survival of hepatocellular carcinoma, tamoxifen-resistant breast cancer, esophageal squamous cell carcinoma, pancreatic adenocarcinoma, colon cancer, and lung adenocarcinoma cell lines and mouse models (21–26).

Studies of ruxolitinib in patients with advanced lung, pancreatic, breast, or colon cancers suggest that this agent is well tolerated, but there are no reports of any significant

improvement in overall survival or progression-free survival (7,27–31). The impact of ruxolitinib has not been reported to date in HNSCC patients.

In the present study, we investigated the impact of ruxolitinib in HNSCC preclinical models, including PDXs generated from HNSCC tumors resected from patients enrolled on a window-of-opportunity trial (NCT03153982) of ruxolitinib to assess whether these models can serve as avatars of clinical response to treatment. Ruxolitinib consistently inhibited STAT3 activation, cell growth and colony formation in HNSCC cell lines. *In vivo*, ruxolitinib treatment inhibited tumor growth in a PDX derived from a patient who exhibited a clinical response in conjunction with decreased STAT3 activation, but not in a PDX from a patient whose disease progressed on ruxolitinib therapy and where STAT3 activation levels were not inhibited by treatment. In addition, baseline levels of pSTAT3 and total STAT3 were higher in the PDX developed from the patient whose disease progressed on therapy. Collectively, our findings indicate that ruxolitinib abrogates JAK/STAT signaling in HNSCC preclinical models suggesting that ruxolitinib treatment may be effective in a subset of HNSCC patients. Assessment of baseline pSTAT3 and total STAT3 levels may be useful for identifying the subset of patients most likely to respond to ruxolitinib.

Materials and Methods

Cell lines

CAL-33, CAL 27 and FaDu cells were purchased from the American Type Culture Collection (ATCC). Cells were cultured in DMEM, 10% fetal bovine serum (FBS) and 1% penicillin-streptomycin (P/S), and maintained at 37 °C with 5% CO_2. All cell lines were authenticated via Short Tandem Repeat (STR) testing using Genetica DNA Laboratories (Burlington, NC, USA).

Antibodies and reagents

The primary antibodies against GAPDH (#5174S), pSTAT3 (#9145S), and total STAT3 (#4904S) were from Cell Signaling Technology (Beverly, MA, USA). Goat anti-rabbit IgG (H + L)-HRP conjugate antibody (#1706515) and Protein Assay Dye Reagent Concentrate (#5000006) were obtained from BioRad (Hercules, CA, USA). PhosSTOP phosphatase inhibitor cocktail tablet (#04906837001) and cOmplete protease inhibitor cocktail tablets (#11697498007) were purchased from Roche Diagnostics (Risch-Rotkreuz, Switzerland). Luminol reagent (#SC-2048) was purchased from Santa Cruz Biotechnology Inc (Dallas, TX, USA). SuperSignal ELISA Femto Maximum (#37075) was purchased from Thermo Scientific Pierce (Waltham, MA, USA). Thiazolyl blue tetrazolium (MTT) (#M5655) was purchased from Sigma Aldrich (St. Louis, MO, USA). One gram of MTT was diluted in 500 mL of phosphate-buffered saline (PBS) and filtered to make a stock solution, then stored at 4 °C. Ruxolitinib was provided by Incyte (Wilmington, DE, USA) in powder form under a Material Transfer Agreement. For cell line experiments, ruxolitinib was dissolved in DMSO to generate a 20 mM stock solution, aliquoted and stored at −20 °C. For *in vivo* experiments, ruxolitinib was dissolved in vehicle (0.5% methyl cellulose and 0.1% tween-80) and stored for up to one week at 4 °C.

Immunoblotting

Cells were plated at 3.0 x 10^5 cells/well in six-well plates and treated the following day with ruxolitinib for 24 hours. The treated cells were harvested using RIPA buffer (150 mM NaCl, 5 mM EDTA, 50 mM Tris pH 8.0, 1% NP-40, 0.5% sodium deoxycholate, 0.1% SDS) with phosSTOP phosphatase inhibitor cocktail and cOmplete protease inhibitor cocktail. Proteins (40 μg/lane) were electrophoresed on 10% SDS/polyacrylamide gels and transferred to polyvinylidene difluoride (PVDF) membranes, blocked for one hour at room temperature in Tris- buffered saline containing 0.1% Tween-20 (TBST) and 5% milk powder, incubated in primary antibodies overnight at 4 °C, then incubated with goat anti-rabbit horse radish peroxidase secondary antibody for one hour at room temperature. Immunoreactive bands were visualized using chemiluminescence and densitometry was performed using ImageJ software.

Cell growth assays

Cells were seeded at 2.0 x 10^4 cells/well in 24-well plates. The cells were treated in triplicate at less than 30% confluence with varying concentrations of ruxolitinib in 5% FBS growth media. All control groups were treated with 0.01% DMSO. After 96 hours of treatment, MTT assays were performed according to the manufacturer's instructions.

Colony formation assays

CAL-33 cells were seeded at 1.0 x 10^3 cells/well in 12-well plates. The next day, cells were treated in triplicate with 3 and 10 μM of ruxolitinib in 5% FBS growth media (25,32). All control groups were treated with vehicle (0.01% DMSO). Drug-containing media was changed every four days. After 11 days, colonies were stained with crystal violet. Colonies were identified and counted using ImageJ software if they were 20 pixels or greater.

Generation and treatment of PDX models

All *in vivo* studies with mouse models were approved by the UCSF Institutional Animal Care and Use Committee (protocol #AN187611). A previously published PDX responsive to AZD1480 was passaged into both flanks of ten 5-6 week-old NOD.Cg-Prkdcscid Il2rgtm1Wjl/SzJ (NSG) mice from The Jackson Laboratory (Bar Harbor, ME, USA) (19). PDX models generated from tumor specimens obtained from ruxolitinib-treated HNSCC patients were derived under the auspices of an ongoing Phase 0 clinical trial (NCT03153982). For PDX models, tumors were resected in the operating room and, after pathologic assessment, a portion was placed in RPMI 1640 media (4 °C) and immediately implanted into both flanks of 5 to 6- week-old NSG mice, as previously described (19). After development, each PDX tumor was passaged into both flanks of 10 NSG mice. When the volumes of PDX tumors reached approximately 150 mm^3, mice were randomized to be treated with vehicle or 75 mg/kg of ruxolitinib, five days per week via oral gavage. Treatment was continued through day 22. Tumors were measured with digital calipers two to three times per week and volumes calculated using the formula: (length x width x width)/2. Mice were euthanized at indicated time points and tumors harvested. Tumor portions used for immunoblotting were frozen at −80 °C; lysates were prepared by extracting protein with a tissue grinder and lysis buffer. Immunoblotting was performed as described above.

The AZD-sensitive PDX was used in the 7th passage, the ruxolitinib progressive disease PDX was used in the 5th passage and the ruxolitinib stable disease PDX was used in the 2nd passage.

Generation and treatment of PDXO models

For air-liquid interface (ALI) cultures, primary organoids were initiated from minced PDX tumor tissue fragments and embedded in type I collagen gels in an inner transwell insert. Culture medium in an outer dish diffused via the permeable transwell into the inner dish and the top of the collagen layer was exposed to air, allowing cells access to a sufficient oxygen supply. Organoid culture medium consisted of Advanced DMEM/F-12 + 10% FBS, supplemented with growth factors including WNT3A, EGF, NOGGIN, and RSPO1. PDXOs were treated with ruxolitinib at selected concentrations (3, 10, 30 μM) or DMSO control for 7 days, followed by evaluation of organoid viability. Briefly, the organoid samples were dissociated with 200 units/mL collagenase IV at 37°C for 45 min, followed by 50 μg/mL Liberase TL for 15 min. The dissociated organoid cells were washed with 100% FBS and resuspended in organoid culture medium. The organoid cells were stained with trypan blue dye to determine the number of live organoids.

Clinical Trial

The parent clinical trial is ongoing at the University of California San Francisco (San Francisco, CA) and the University of Arizona (Tucson, AZ). The protocol was approved by both local institutional review boards, carried out in accordance with the Declaration of Helsinki and Good Clinical Practice, and registered with ClinicalTrials.gov (NCT03153982). All patients gave written informed consent. Key eligibility criteria included: primary or recurrent HNSCC planned for oncologic surgery; age ≥ 18; ECOG performance status 0-2; adequate end-organ function. Participants are treated with ruxolitinib 20 mg twice daily for 14-28 days from enrollment to the morning of surgery. Given the brief duration on therapy, we used the quantitative change in tumor size as a more informative continuous variable against which to assess biomarkers in our prior window-of-opportunity trials (33,34). The RECIST system was used to define index lesions and the sum longest diameter.

Statistical Analysis

Densitometry data was analyzed using generalized linear models, if required to meet the assumptions of the models, on the log transformed scale. Statistical significance of the ratio of pSTAT3 to total STAT3 between the vehicle- and ruxolitinib-treated groups was determined via contrasts with the multiplicity of comparisons adjusted to control the experiment-wise type I error rate at 5%. When multiple doses of ruxolitinib were considered, the step-down Holm method was used to control the overall type I error rate within each experiment (35). When only one dose was considered and comparing the treatment group comparisons conducted for progressive and stable disease PDXs was the focus, the Bonferroni method was used. For *in vivo* xenograft experiments, random effects models were used to address variation in the tumor growth rate across the mice within the xenograft experiments. Data was log-transformed to meet the assumptions of the random effects models. Statistical significance of the comparison of total tumor volume change from

baseline (fold change on the log scale) was determined via contrasts. For *ex vivo* organoids experiments, the unpaired two-samples t-test was used to compare the mean of organoids derived from progressive and stable disease PDXs. All statistical analyses were performed using sas software version 9.3 (SAS institute, Cary, NC, USA) at a significance level of 0.05.

Results

Ruxolitinib inhibits STAT3 activation in HNSCC cell lines

We previously reported that the JAK inhibitor AZD1480 abrogated STAT3 activation in HNSCC cells (19). To assess the impact of ruxolitinib inhibition of JAK1/2 on STAT3 activation, a panel of representative HNSCC cell lines, CAL-33, CAL 27, and FaDu, were treated with increasing doses of ruxolitinib for 24 hours. Expression levels of total and phosphorylated STAT3 levels were assessed via immunoblotting and the pSTAT3/total STAT3 ratio quantified by densitometry. As shown in Figure 1, ruxolitinib treatment resulted in a dose-dependent decrease of pSTAT3 levels in all three HNSCC cell lines, and the decrease was significant when the ruxolitinib dose was ≥ 0.1μM.

Ruxolitinib inhibits HNSCC cell growth

Activated STAT3 induces the transcription of pro-proliferative genes. Aberrant or constitutive STAT3 activation can therefore lead to unregulated cell growth, a hallmark of cancer (36,37). To determine whether ruxolitinib inhibition of JAK1/2 abrogates HNSCC cell growth, CAL-33, CAL 27, and FaDu cells (selected because they have been extensively characterized, are widely available, and exhibit STAT3 activation upon cytokine stimulation) were treated for 96 hours with vehicle or increasing doses of ruxolitinib in three separate experiments, followed by performance of MTT assays. Inhibition of cellular growth (relative to vehicle treatment) was observed in the HNSCC cell lines at higher doses of ruxolitinib (Figure 2a).

Ruxolitinib decreases colony-forming ability of HNSCC cells

Colony formation is another approach to test the impact of a drug on tumor cell proliferation and survival. To investigate the impact of ruxolitinib on the colony-forming ability of HNSCC cells, CAL-33 cells were treated with two different concentrations (3 and 10 μM) of ruxolitinib in two independent experiments. At the end of the treatment period, colonies were stained with crystal violet and quantified. Decreased colony number was observed with 10 μM ruxolitinib treatment ($P = 0.0001$). (Figure 2b).

Ruxolitinib abrogates growth of HNSCC PDX previously responsive to AZD1480

Given the promising *in vitro* results in HNSCC cell lines, xenograft models were generated in immunodeficient mice to assess the impact of ruxolitinib treatment on tumor growth *in vivo*. We previously reported that HNSCC PDX growth was inhibited by treatment with AZD1480, a JAK inhibitor whose clinical development was halted due to neurotoxicity in early phase trials (18–20). Thus, we investigated whether ruxolitinib, a safe and well-tolerated JAK1/2 inhibitor, demonstrates comparable efficacy in this same PDX model. As shown in Figure 3a, ruxolitinib significantly slowed tumor growth in the AZD1480-sensitive

HNSCC PDX model ($P = 0.0082$). For all *in vivo* studies of ruxolitinib, we selected a dose based on previous reports in tumor xenografts (38,39). To determine the impact of ruxolitinib on STAT3 activation in the tumors, the levels of pSTAT3 in tumor lysates were determined by immunoblotting. Ruxolitinib treatment significantly decreased pSTAT3 levels ($P = 0.0008$) in the PDXs in conjunction with abrogation of tumor growth.

Ruxolitinib impact on STAT3 and tumor growth in HNSCC PDXs and PDXOs from patients treated on a window-of-opportunity trial

A window-of-opportunity clinical trial (NCT03153982) is ongoing to evaluate the pharmacodynamic impact of ruxolitinib in HNSCC. Tumor volumes before and after treatment are calculated according to RECIST 1.1 criteria and compared (33). Given the short duration of treatment, we describe the proportion of patients whose tumor volumes decrease or increase as defined previously (34,40). In these earlier window-of-opportunity trials, we elected not to use RECIST definitions, since the short window of exposure is unlikely to result in a partial response. We defined the quantitative change in tumor size as a more informative continuous variable. PDXs were generated from the post-treatment samples as we have described previously (19).

In order to determine whether clinical responses observed in the window setting were concordant in the PDX models generated from post-treatment tumors, we selected two post-treatment PDXs from a representative patient with stable disease vs. one with progressive disease on ruxolitinib treatment (exhibited >20% increase in sum longest diameter of index lesion) (Table 1). The patient whose HNSCC progressed was a 71-year-old woman with a T2N0M0 (stage 2) human papilloma virus (HPV)-negative cancer of the oral tongue who received 15 days of ruxolitinib treatment. The patient whose tumor did not progress on ruxolitinib was a 57-year- old woman with a T3N2bM0 (stage 4) HPV-negative cancer of the oral tongue who was treated for 18 days with ruxolitinib prior to surgical resection (exhibited no change in sum longest diameter of index lesion). The PDXs were randomized to be treated with either vehicle or ruxolitinib for 3 weeks.

As shown in Figure 4a, tumors grew approximately linearly on the log-transformed scale within each mouse. We analyzed longitudinal measurements of total tumor volume on the log- transformed scale using a random effects model. The model accommodates between mouse heterogeneity and permits different lines (different intercepts/slopes) to approximate longitudinal change in total tumor volume within the mice. The impact of ruxolitinib on tumor growth is represented as the difference in the average slope (average rate of tumor growth) by treatment. For the ruxolitinib progressive disease PDX, it took 35 days for the tumors to achieve 150 mm^3; for the ruxolitinib stable disease PDX, it took 20 days for the tumors to achieve 150 mm^3.The mice with tumors were randomized into vehicle and ruxolitinib groups when the average tumor volume reached about 150 mm^3.

Ruxolitinib significantly inhibited tumor growth in the PDX from the patient who demonstrated SD on treatment ($P = 0.0001$). In contrast, ruxolitinib did not inhibit growth of the PDX derived from the patient who experienced PD on therapy ($P = 0.7599$). However, in the absence of PDX models developed from the pre-ruxolitinib treated tumors, it is not

possible to determine the role of ruxolitinib treatment in the apparent resistance of the patient with PD.

We did not detect any significant difference in the tumor histology of the two representative patients enrolled on the ruxolitinib clinical trial (Supplemental Figure 1). Both patients' tissue sections showed a keratinizing, well to moderately differentiated squamous cell carcinoma. A pre-treatment tumor sample was only available for one of the patients (SD) and while there was no histologic evidence of tumor regression, the post-treatment excision showed slightly more atypia compared with the pre-treatment biopsy with scattered foci of moderately differentiated tumor. The degree of inflammation in the two post-treatment tumors was similar. When comparing the clinical patient samples to the PDX tissues, the histology was very similar. The only significant histologic differences between the patient tissue and the PDX tissue are that the clinical specimen also contains a mild chronic inflammatory infiltrate.

To determine whether ruxolitinib treatment impacted STAT3 activation, pSTAT3 levels in the PD and SD PDX tumor specimens were analyzed by immunoblotting. As shown in Figure 4b, while downregulation of pSTAT3 by ruxolitinib treatment was observed in both PDXs, inhibition of STAT3 activation was more pronounced in the PDX from the patient whose tumor did not grow in the neoadjuvant setting with ruxolitinib treatment (adjusted *P* value of 0.0532 for the PD PDX and 0.0174 for the SD PDX). Unexpectedly, pSTAT3 levels were increased by ruxolitinib treatment in the PDX derived from the patient whose disease progressed on therapy. Comparison of baseline pSTAT3 levels in the vehicle group PDX tumors (using the same lysates to generate the results in panel 4b) revealed higher expression in the PDX derived from the patient whose disease progressed compared with the PDX from the patient whose disease was stable on ruxolitinib treatment ($P = 0.0001$; Figure 4c). Similarly, baseline levels of total STAT3 were higher in the PD PDX compared to the SD PDX ($P = 0.0123$; Figure 4c). These results suggest that baseline levels of either pSTAT3 or total STAT3 may serve as predictive biomarkers to identify patients who are likely to respond to ruxolitinib therapy.

To confirm our findings using an *ex vivo* approach, we generated organoids from the PDXs and tested the impact of ruxolitinib. As shown in Figure 5, ruxolitinib demonstrated a dose-dependent decrease in cell growth, as measured by vital dye exclusion, in the organoids derived from a patient who experienced the stable disease (SD) clinical response compared to organoids derived from a patient who demonstrated progressive disease (PD). Similar results were seen using a metabolic assay (Supplemental Figure 3). As observed with the PDX experiments, pSTAT3 expression levels were downregulated in the PDX-derived organoids from the patient with SD compared to the organoids from the patient with PD (Supplemental Figure 2). These results suggest that antitumor effects can be tested without requiring the use of additional laboratory animals.

Discussion

Aberrant hyperactivation of STAT3 is associated with disease progression and poor prognosis in HNSCC (2,41). Directly targeting STAT3 has been challenging, and the

possibility of targeting upstream activators such as JAKs with small molecule inhibitors represents an attractive alternative (3). JAK inhibition with AZD1480 in HNSCC preclinical models showed promising *in vitro* and *in vivo* results; however, neurotoxicity detected in a Phase I trial halted the clinical development of this agent (19,20). Ruxolitinib is a selective JAK1/2 inhibitor that was approved by the FDA for myeloproliferative disorders—many of which are associated with an activating JAK2 V617F mutation—after it was shown to decrease STAT3 activation and symptom burden in these hematological malignancies (14,16,42). However, its efficacy in solid tumors, including HNSCC, is incompletely understood. We evaluated the anti-cancer effects of ruxolitinib in HNSCC preclinical models including PDXs generated from patients treated with ruxolitinib in an ongoing window-of-opportunity clinical trial.

Preclinical studies investigating JAK inhibition with ruxolitinib in a variety of solid tumors, including HNSCC, have shown promising anti-cancer effects. Treatment of hepatocellular carcinoma cell lines with ruxolitinib inhibited STAT3 activation and cell proliferation and survival at higher concentrations than used in the present study (25). Similar abrogation of STAT3 activation was observed in pancreatic adenocarcinoma and colon cancer cell lines (23,24). In esophageal squamous cell carcinoma, ruxolitinib treatment inhibited STAT3 activation and decreased cell proliferation in a dose-dependent manner (26). Others reported that ruxolitinib treatment abrogated STAT3 phosphorylation in HNSCC CAL 27 cells, consistent with our results using this cell line (43). In the HNSCC cell line SCC15, ruxolitinib treatment reduced cell growth (44). Overall, our results provide further evidence that ruxolitinib abrogates STAT3 activation and inhibits tumor growth in solid tumor preclinical models, including HNSCC.

Several *in vivo* studies in solid tumors have demonstrated that ruxolitinib inhibits tumor growth and decreases pSTAT3 levels in cell line-derived xenografts and PDXs. Mice harboring non-small cell lung cancer xenografts treated with ruxolitinib, alone or in combination with cisplatin, exhibited significant abrogation of STAT3 activation and inhibition of tumor growth, compared to the control group (45,46). The impact of ruxolitinib has been tested *in vivo* using HNSCC cell line-derived tumor models as well; mice harboring HNSCC tumors derived from SCC9 cells were treated with ruxolitinib. However, there was no effect on tumor growth and proliferation (44). In addition to the PDXs reported in this study, the impact of ruxolitinib on solid tumors has been reported previously in five hepatocellular carcinoma PDXs models. These hepatocellular carcinoma PDX models were generated from tumors with wild-type JAK1 or mutant JAK1 (S703I, N451S, E483D, and A1066S mutations) (47). Of these models, only JAK1 S703I represents an activating mutation; ruxolitinib treatment of this PDX model resulted in a significant inhibition of tumor growth and STAT3 activation (47). In contrast, ruxolitinib treatment of the three PDXs with the non-activating JAK1 mutations did not evoke anti-tumor effects (47). While ruxolitinib has not previously been tested in HNSCC PDXs, we reported that treatment with the JAK1/2 inhibitor AZD1480 resulted in inhibition of STAT3 activation and tumor growth in HNSCC PDXs (19). In the present study, the same AZD1480-responsive HNSCC PDX also exhibited decreased tumor growth and reduced STAT3 activation after three weeks of ruxolitinib treatment.

The anti-tumor effects of ruxolitinib are being studied in a variety of hematological malignancies and solid tumors, as well as PDXs derived from ruxolitinib-treated patients. In a Phase I/II single-arm clinical trial investigating the impact of ruxolitinib on chronic myelomonocytic leukemia (CMML), 36% of enrolled patients responded to treatment, and 40% of patients with splenomegaly had greater than a 50% reduction in splenic size (NCT01776723) (48). PDX models were generated using pre-treatment bone marrow mononuclear cells from three responders and three non-responders with splenomegaly in order to determine whether responses to ruxolitinib treatment in these models recapitulated findings in the clinical trial. Ruxolitinib-treated PDXs from clinical responders had a significant reduction in spleen and engraftment size compared to vehicle-treated PDXs; this impact was not observed in PDXs from clinical non-responders. Similarly, in our study, ruxolitinib treatment of a HNSCC PDX model generated from a HNSCC patient who exhibited SD on neoadjuvant ruxolitinib, resulted in tumor growth inhibition in conjunction with decreased STAT3 activation. In contrast, ruxolitinib failed to abrogate both STAT3 activation and tumor growth in a HNSCC PDX derived from a patient whose disease progressed on ruxolitinib treatment. Increased baseline levels of pSTAT3 and total STAT3 were detected in the PDX developed from the PD patient compared with the SD patient. These findings support the possibility that baseline expression of the pathway targets may serve as predictive biomarkers to identify patients most likely to benefit from ruxolitinib treatment.

Overall, our *in vitro* and *in vivo* findings are consistent with other studies in solid tumor models. However, the relatively high concentrations required to achieve maximum growth inhibition may limit clinical translation of our findings in preclinical models. Our studies with PDX models suggest that ruxolitinib may be effective in a subset of HNSCC patients with this malignancy based on expression of total and/or phosphorylated STAT3. For example, a prior report that ruxolitinib inhibited tumor growth only in hepatocellular carcinoma PDXs that carry an activating JAK mutation (47). Finally, we demonstrate that ruxolitinib treatment of PDXs mirrors the clinical response in patients with HNSCC, which was consistent with a similar study in CMML; to our knowledge a similar finding has not been reported to date in other solid tumors (48).

The immunological impact of JAK inhibition with ruxolitinib in HNSCC is an area for further study as this agent has been shown to have immunosuppressive, with anti-inflammatory effects (49). In patients with myeloproliferative neoplasms, ruxolitinib treatment decreased the number of $CD4^+$ T cells and pro-inflammatory cytokines (50). Its anti-inflammatory impact makes ruxolitinib a potentially attractive therapy for solid tumors as development of these cancers is associated with chronic inflammation, such as through interleukin 6 (IL6)-mediated STAT3 activation (3,51). Furthermore, cytokine secretion from tumors themselves has been shown to inhibit activation of cytotoxic T cells, thereby impeding anti-cancer immune response (51). Treatment of mice harboring pancreatic adenocarcinoma with ruxolitinib not only decreased tumor volume, but also restored cytotoxic T lymphocyte levels in tumors, as evidenced by elevated $CD8^+$ cell levels (52). Further studies on the immunological impact of ruxolitinib in immunocompetent HNSCC models are warranted.

In this study we demonstrated that ruxolitinib exhibits anti-cancer effects in HNSCC *in vitro* and *in vivo* models. Whereas all cell lines tested demonstrated decreased pSTAT3 expression and reduced proliferation upon ruxolitinib treatment, the PDXs derived from patients treated with this agent on a window-of-opportunity are more informative. Our findings in these relevant preclinical models suggest that baseline levels pSTAT3 and total STAT3, as well as modulation of pSTAT3 following a brief course of ruxolitinib, may identify patients most likely to respond to this JAK/STAT inhibitor.

Supplementary Material

Refer to Web version on PubMed Central for supplementary material.

Financial Support:

This work was supported by NIH R35CA231998 (J.R.G.), R01DE028289 (D.E.J. and J.R.G.), and a Yearlong Research Fellowship awarded by the University of California San Francisco School of Medicine (Z.Q.).

Conflicts of Interest Disclosure:

Funding for this study was provided, in part, by Incyte Corporation, the manufacturer of ruxolitinib. Ruxolitinib was provided through a Material Transfer Agreement with Incyte Corporation. Drs. Grandis and Johnson are co-inventors of a decoy oligonucleotide targeting STAT3.

References

1. Rawlings JS, Rosler KM, Harrison DA. The JAK/STAT signaling pathway. J Cell Sci 2004;117(Pt 8):1281–3 doi 10.1242/jcs.00963. [PubMed: 15020666]
2. Grandis JR, Drenning SD, Zeng Q, Watkins SC, Melhem MF, Endo S, et al. Constitutive activation of Stat3 signaling abrogates apoptosis in squamous cell carcinogenesis in vivo. Proc Natl Acad Sci U S A 2000;97(8):4227–32 doi 10.1073/pnas.97.8.4227. [PubMed: 10760290]
3. Johnson DE, O'Keefe RA, Grandis JR. Targeting the IL-6/JAK/STAT3 signalling axis in cancer. Nat Rev Clin Oncol 2018;15(4):234–48 doi 10.1038/nrclinonc.2018.8. [PubMed: 29405201]
4. Macha MA, Matta A, Kaur J, Chauhan SS, Thakar A, Shukla NK, et al. Prognostic significance of nuclear pSTAT3 in oral cancer. Head Neck 2011;33(4):482–9 doi 10.1002/hed.21468. [PubMed: 20652980]
5. Yadav A, Kumar B, Datta J, Teknos TN, Kumar P. IL-6 promotes head and neck tumor metastasis by inducing epithelial-mesenchymal transition via the JAK-STAT3-SNAIL signaling pathway. Mol Cancer Res 2011;9(12):1658–67 doi 10.1158/1541-7786.MCR-11-0271. [PubMed: 21976712]
6. Sabanés Zariquiey F, Da Souza JV, Estrada-Tejedor R & Bronowska AK If You Cannot Win Them, Join Them: Understanding New Ways to Target STAT3 by Small Molecules. ACS Omega 2019;4:13913–21. [PubMed: 31497709]
7. Hurwitz HI, Uppal N, Wagner SA, Bendell JC, Beck JT, Wade SM, 3rd, et al. Randomized, Double-Blind, Phase II Study of Ruxolitinib or Placebo in Combination With Capecitabine in Patients With Metastatic Pancreatic Cancer for Whom Therapy With Gemcitabine Has Failed. J Clin Oncol 2015;33(34):4039–47 doi 10.1200/JCO.2015.61.4578. [PubMed: 26351344]
8. Fleischmann R, Kremer J, Cush J, Schulze-Koops H, Connell CA, Bradley JD, et al. Placebo-controlled trial of tofacitinib monotherapy in rheumatoid arthritis. N Engl J Med 2012;367(6):495–507 doi 10.1056/NEJMoa1109071. [PubMed: 22873530]
9. Furumoto Y, Gadina M. The arrival of JAK inhibitors: advancing the treatment of immune and hematologic disorders. BioDrugs 2013;27(5):431–8 doi 10.1007/s40259-013-0040-7. [PubMed: 23743669]

10. Sandborn WJ, Su C, Sands BE, D'Haens GR, Vermeire S, Schreiber S, et al. Tofacitinib as Induction and Maintenance Therapy for Ulcerative Colitis. N Engl J Med 2017;376(18):1723–36 doi 10.1056/NEJMoa1606910. [PubMed: 28467869]
11. Wernig G, Kharas MG, Okabe R, Moore SA, Leeman DS, Cullen DE, et al. Efficacy of TG101348, a selective JAK2 inhibitor, in treatment of a murine model of JAK2V617F- induced polycythemia vera. Cancer Cell 2008;13(4):311–20 doi 10.1016/j.ccr.2008.02.009. [PubMed: 18394554]
12. Harrison C, Kiladjian JJ, Al-Ali HK, Gisslinger H, Waltzman R, Stalbovskaya V, et al. JAK inhibition with ruxolitinib versus best available therapy for myelofibrosis. N Engl J Med 2012;366(9):787–98 doi 10.1056/NEJMoa1110556. [PubMed: 22375970]
13. Harrison CN, Schaap N, Vannucchi AM, Kiladjian JJ, Tiu RV, Zachee P, et al. Janus kinase-2 inhibitor fedratinib in patients with myelofibrosis previously treated with ruxolitinib (JAKARTA-2): a single-arm, open-label, non-randomised, phase 2, multicentre study. Lancet Haematol 2017;4(7):e317–e24 doi 10.1016/S2352-3026(17)30088-1. [PubMed: 28602585]
14. Kralovics R, Passamonti F, Buser AS, Teo SS, Tiedt R, Passweg JR, et al. A gain-of- function mutation of JAK2 in myeloproliferative disorders. N Engl J Med 2005;352(17):1779–90 doi 10.1056/NEJMoa051113. [PubMed: 15858187]
15. Pardanani A, Harrison C, Cortes JE, Cervantes F, Mesa RA, Milligan D, et al. Safety and Efficacy of Fedratinib in Patients With Primary or Secondary Myelofibrosis: A Randomized Clinical Trial. JAMA Oncol 2015;1(5):643–51 doi 10.1001/jamaoncol.2015.1590. [PubMed: 26181658]
16. Shi JG, Chen X, McGee RF, Landman RR, Emm T, Lo Y, et al. The pharmacokinetics, pharmacodynamics, and safety of orally dosed INCB018424 phosphate in healthy volunteers. J Clin Pharmacol 2011;51(12):1644–54 doi 10.1177/0091270010389469. [PubMed: 21257798]
17. Zhang M, Xu CR, Shamiyeh E, Liu F, Yin JY, von Moltke LL, et al. A randomized, placebo-controlled study of the pharmacokinetics, pharmacodynamics, and tolerability of the oral JAK2 inhibitor fedratinib (SAR302503) in healthy volunteers. J Clin Pharmacol 2014;54(4):415–21 doi 10.1002/jcph.218. [PubMed: 24165976]
18. Hedvat M, Huszar D, Herrmann A, Gozgit JM, Schroeder A, Sheehy A, et al. The JAK2 inhibitor AZD1480 potently blocks Stat3 signaling and oncogenesis in solid tumors. Cancer Cell 2009;16(6):487–97 doi 10.1016/j.ccr.2009.10.015. [PubMed: 19962667]
19. Sen M, Pollock NI, Black J, DeGrave KA, Wheeler S, Freilino ML, et al. JAK kinase inhibition abrogates STAT3 activation and head and neck squamous cell carcinoma tumor growth. Neoplasia 2015;17(3):256–64 doi 10.1016/j.neo.2015.01.003. [PubMed: 25810010]
20. Plimack ER, Lorusso PM, McCoon P, Tang W, Krebs AD, Curt G, et al. AZD1480: a phase I study of a novel JAK2 inhibitor in solid tumors. Oncologist 2013;18(7):819–20 doi 10.1634/theoncologist.2013-0198. [PubMed: 23847256]
21. Kim JW, Gautam J, Kim JE, Kim JA, Kang KW. Inhibition of tumor growth and angiogenesis of tamoxifen-resistant breast cancer cells by ruxolitinib, a selective JAK2 inhibitor. Oncol Lett 2019;17(4):3981–9 doi 10.3892/ol.2019.10059. [PubMed: 30930994]
22. Lee S, Shah T, Yin C, Hochberg J, Ayello J, Morris E, et al. Ruxolitinib significantly enhances in vitro apoptosis in Hodgkin lymphoma and primary mediastinal B-cell lymphoma and survival in a lymphoma xenograft murine model. Oncotarget 2018;9(11):9776–88 doi 10.18632/oncotarget.24267. [PubMed: 29515770]
23. Radhakrishnan H, Ilm K, Walther W, Shirasawa S, Sasazuki T, Daniel PT, et al. MACC1 regulates Fas mediated apoptosis through STAT1/3 - Mcl-1 signaling in solid cancers. Cancer Lett 2017;403:231–45 doi 10.1016/j.canlet.2017.06.020. [PubMed: 28649004]
24. Smigiel JM, Parameswaran N, Jackson MW. Potent EMT and CSC Phenotypes Are Induced By Oncostatin-M in Pancreatic Cancer. Mol Cancer Res 2017;15(4):478–88 doi 10.1158/1541-7786.MCR-16-0337. [PubMed: 28053127]
25. Wilson GS, Tian A, Hebbard L, Duan W, George J, Li X, et al. Tumoricidal effects of the JAK inhibitor Ruxolitinib (INC424) on hepatocellular carcinoma in vitro. Cancer Lett 2013;341(2):224–30 doi 10.1016/j.canlet.2013.08.009. [PubMed: 23941832]
26. Yang PW, Huang PM, Yong LS, Chang YH, Wu CW, Hua KT, et al. Circulating Interleukin-6 is Associated with Prognosis and Genetic Polymorphisms of MIR608 in Patients with

Esophageal Squamous Cell Carcinoma. Ann Surg Oncol 2018;25(8):2449– 56 doi 10.1245/s10434-018-6532-4. [PubMed: 29948421]

27. Fogelman D, Cubillo A, Garcia-Alfonso P, Miron MLL, Nemunaitis J, Flora D, et al. Randomized, double-blind, phase two study of ruxolitinib plus regorafenib in patients with relapsed/refractory metastatic colorectal cancer. Cancer Med 2018;7(11):5382–93 doi 10.1002/cam4.1703. [PubMed: 30123970]
28. Giaccone G, Sanborn RE, Waqar SN, Martinez-Marti A, Ponce S, Zhen H, et al. A Placebo-Controlled Phase II Study of Ruxolitinib in Combination With Pemetrexed and Cisplatin for First-Line Treatment of Patients With Advanced Nonsquamous Non-Small- Cell Lung Cancer and Systemic Inflammation. Clin Lung Cancer 2018;19(5):e567–e74 doi 10.1016/j.cllc.2018.03.016. [PubMed: 29681434]
29. Hurwitz H, Van Cutsem E, Bendell J, Hidalgo M, Li CP, Salvo MG, et al. Ruxolitinib + capecitabine in advanced/metastatic pancreatic cancer after disease progression/intolerance to first-line therapy: JANUS 1 and 2 randomized phase III studies. Invest New Drugs 2018;36(4):683–95 doi 10.1007/s10637-018-0580-2. [PubMed: 29508247]
30. O'Shaughnessy J, DeMichele A, Ma CX, Richards P, Yardley DA, Wright GS, et al. A randomized, double-blind, phase 2 study of ruxolitinib or placebo in combination with capecitabine in patients with advanced HER2-negative breast cancer and elevated C- reactive protein, a marker of systemic inflammation. Breast Cancer Res Treat 2018;170(3):547–57 doi 10.1007/s10549-018-4770-6. [PubMed: 29675680]
31. Yu HA, Perez L, Chang Q, Gao SP, Kris MG, Riely GJ, et al. A Phase 1/2 Trial of Ruxolitinib and Erlotinib in Patients with EGFR-Mutant Lung Adenocarcinomas with Acquired Resistance to Erlotinib. J Thorac Oncol 2017;12(1):102–9 doi 10.1016/j.jtho.2016.08.140. [PubMed: 27613527]
32. Franken NA, Rodermond HM, Stap J, Haveman J, van Bree C. Clonogenic assay of cells in vitro. Nat Protoc 2006;1(5):2315–9 doi 10.1038/nprot.2006.339. [PubMed: 17406473]
33. Eisenhauer EA, Therasse P, Bogaerts J, Schwartz LH, Sargent D, Ford R, et al. New response evaluation criteria in solid tumours: revised RECIST guideline (version 1.1). Eur J Cancer 2009;45(2):228–47 doi 10.1016/j.ejca.2008.10.026. [PubMed: 19097774]
34. Bauman JE, Duvvuri U, Gooding WE, Rath TJ, Gross ND, Song J, et al. Randomized, placebo-controlled window trial of EGFR, Src, or combined blockade in head and neck cancer. JCI Insight 2017;2(6):e90449 doi 10.1172/jci.insight.90449. [PubMed: 28352657]
35. Holm S A simple sequentially rejective multiple test procedure. Scand J Statist 1979;6:65–70.
36. Alvarez JV, Frank DA. Genome-wide analysis of STAT target genes: elucidating the mechanism of STAT-mediated oncogenesis. Cancer Biol Ther 2004;3(11):1045–50 doi 10.4161/cbt.3.11.1172. [PubMed: 15539936]
37. Hanahan D, Weinberg RA. The hallmarks of cancer. Cell 2000;100(1):57–70 doi 10.1016/s0092-8674(00)81683-9. [PubMed: 10647931]
38. Reeves PM, Abbaslou MA, Kools FRW, Vutipongsatorn K, Tong X, Gavegnano C, et al. Ruxolitinib sensitizes ovarian cancer to reduced dose Taxol, limits tumor growth and improves survival in immune competent mice. Oncotarget 2017;8(55):94040–53 doi 10.18632/oncotarget.21541. [PubMed: 29212208]
39. Heine A, Held SA, Daecke SN, Wallner S, Yajnanarayana SP, Kurts C, et al. The JAK- inhibitor ruxolitinib impairs dendritic cell function in vitro and in vivo. Blood 2013;122(7):1192–202 doi 10.1182/blood-2013-03-484642. [PubMed: 23770777]
40. Duvvuri U, George J, Kim S, Alvarado D, Neumeister VM, Chenna A, et al. Molecular and Clinical Activity of CDX-3379, an Anti-ErbB3 Monoclonal Antibody, in Head and Neck Squamous Cell Carcinoma Patients. Clin Cancer Res 2019;25(19):5752–8 doi 10.1158/1078-0432.CCR-18-3453. [PubMed: 31308059]
41. Lui VW, Peyser ND, Ng PK, Hritz J, Zeng Y, Lu Y, et al. Frequent mutation of receptor protein tyrosine phosphatases provides a mechanism for STAT3 hyperactivation in head and neck cancer. Proc Natl Acad Sci U S A 2014;111(3):1114–9 doi 10.1073/pnas.1319551111. [PubMed: 24395800]

42. Verstovsek S, Mesa RA, Gotlib J, Levy RS, Gupta V, DiPersio JF, et al. A double-blind, placebo-controlled trial of ruxolitinib for myelofibrosis. N Engl J Med 2012;366(9):799–807 doi 10.1056/NEJMoa1110557. [PubMed: 22375971]
43. Chang WM, Chang YC, Yang YC, Lin SK, Chang PM, Hsiao M. AKR1C1 controls cisplatin-resistance in head and neck squamous cell carcinoma through cross-talk with the STAT1/3 signaling pathway. J Exp Clin Cancer Res 2019;38(1):245 doi 10.1186/s13046-019-1256-2. [PubMed: 31182137]
44. Vallath S, Sage EK, Kolluri KK, Lourenco SN, Teixeira VS, Chimalapati S, et al. CADM1 inhibits squamous cell carcinoma progression by reducing STAT3 activity. Sci Rep 2016;6:24006 doi 10.1038/srep24006. [PubMed: 27035095]
45. Hu Y, Hong Y, Xu Y, Liu P, Guo DH, Chen Y. Inhibition of the JAK/STAT pathway with ruxolitinib overcomes cisplatin resistance in non-small-cell lung cancer NSCLC. Apoptosis 2014;19(11):1627–36 doi 10.1007/s10495-014-1030-z. [PubMed: 25213670]
46. Mohrherr J, Haber M, Breitenecker K, Aigner P, Moritsch S, Voronin V, et al. JAK-STAT inhibition impairs K-RAS-driven lung adenocarcinoma progression. Int J Cancer 2019;145(12):3376–88 doi 10.1002/ijc.32624. [PubMed: 31407334]
47. Yang S, Luo C, Gu Q, Xu Q, Wang G, Sun H, et al. Activating JAK1 mutation may predict the sensitivity of JAK-STAT inhibition in hepatocellular carcinoma. Oncotarget 2016;7(5):5461–9 doi 10.18632/oncotarget.6684. [PubMed: 26701727]
48. Hea Newman. Patient Derived Xenografts (PDX) Recapitulate Ruxolitinib Clinical Trial Responses and Identify a Novel Combination Therapy for Chronic Myelomonocytic Leukemia (CMML). Blood 2019;134:2984-.
49. Elli EM, Barate C, Mendicino F, Palandri F, Palumbo GA. Mechanisms Underlying the Anti-inflammatory and Immunosuppressive Activity of Ruxolitinib. Front Oncol 2019;9:1186 doi 10.3389/fonc.2019.01186. [PubMed: 31788449]
50. Sea Parampalli Yajnanarayana. JAK1/2 inhibition impairs T cell function in vitro and in patients with myeloproliferative neoplasms. Br J Haematol 2015;169:824–33. [PubMed: 25824483]
51. Elinav E, Nowarski R, Thaiss CA, Hu B, Jin C, Flavell RA. Inflammation-induced cancer: crosstalk between tumours, immune cells and microorganisms. Nat Rev Cancer 2013;13(11):759–71 doi 10.1038/nrc3611. [PubMed: 24154716]
52. Lu C, Talukder A, Savage NM, Singh N, Liu K. JAK-STAT-mediated chronic inflammation impairs cytotoxic T lymphocyte activation to decrease anti-PD-1 immunotherapy efficacy in pancreatic cancer. Oncoimmunology 2017;6(3):e1291106 doi 10.1080/2162402X.2017.1291106. [PubMed: 28405527]

Translational Relevance

The role of JAK/STAT inhibitors in the treatment of solid tumors is unknown. HNSCC is characterized by STAT3 hyperactivation in a subset of tumors. In this study, we demonstrate that baseline levels of total and/or phosphorylated STAT3 may serve as predictive biomarkers for treatment with the FDA-approved JAK/STAT inhibitor ruxolitinib in HNSCC patients. Both PDX and organoid models may serve as relevant preclinical models to predict treatment responses for individual patients.

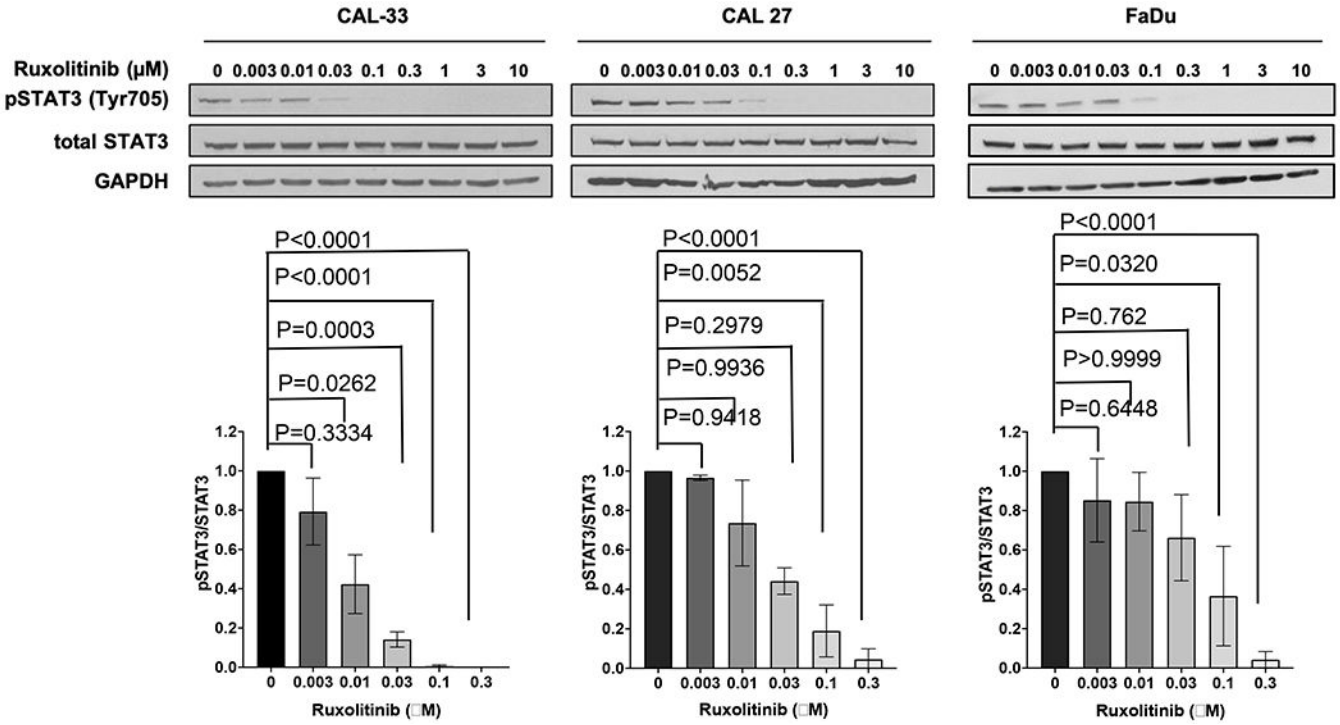

Figure 1. Dose-dependent effects of ruxolitinib on STAT3 activation in HNSCC cell lines.

Levels of pSTAT3 and total STAT3 were assessed in CAL-33, CAL 27, and FaDu cell lines by immunoblot after 24 h of ruxolitinib treatment at the indicated doses. GAPDH was used as a loading control. The ratio of pSTAT3 to total STAT3 was determined by densitometry. Columns depict the averages of the pSTAT3/total STAT3 ratios, normalized to the vehicle within each experiment, from three independent experiments for CAL-33 and FaDu and from two independent experiments for CAL 27 that showed. Statistical significance was determined as described in Materials and Methods with the experiment-wise error rate controlled at 5%.

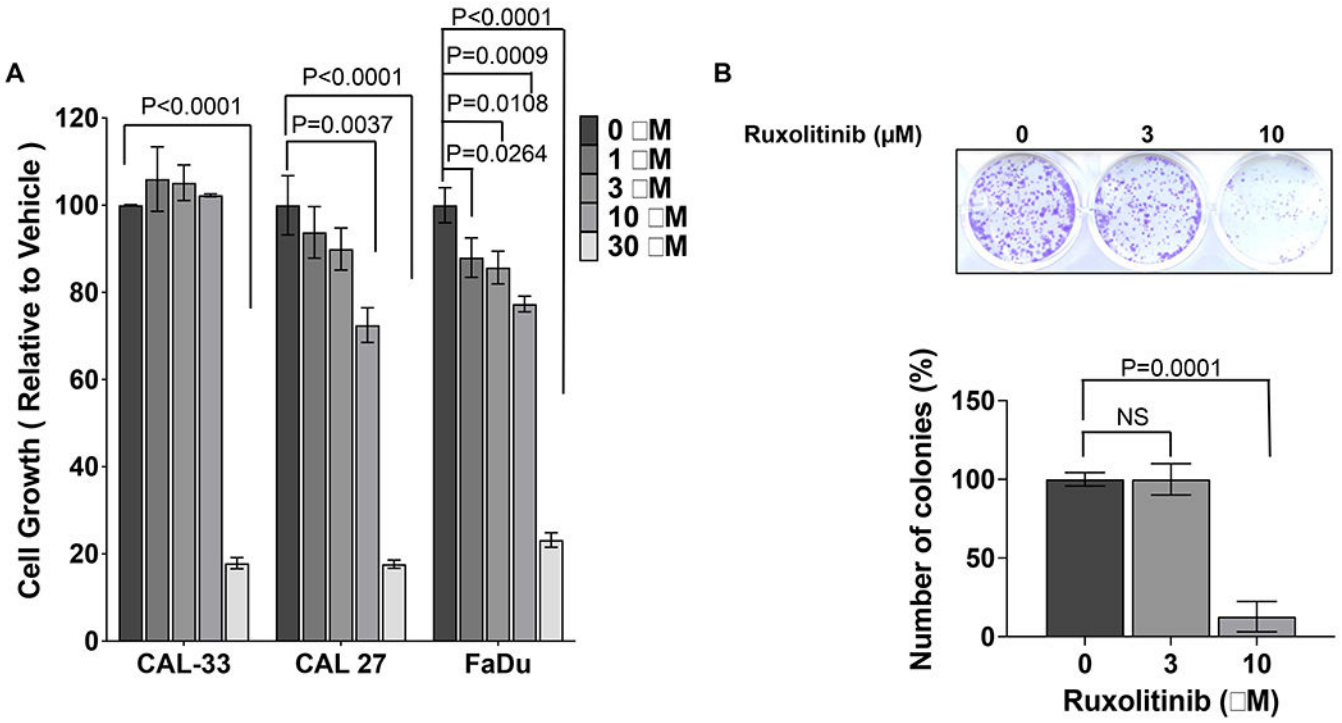

Figure 2. Inhibition of cell growth and colony formation by ruxolitinib.

A. CAL-33, CAL 27, and FaDu cells were plated in triplicate in 24-well plates and treated with the indicated doses of ruxolitinib for 96 hours. Cell growth was determined by MTT assays and comparison of absorbance at each dose with that of the vehicle-treated group for each cell line. Columns represent the average of three biological replicates for a given dose, and error bars represent standard deviation. The experiment was performed three times with similar results. **B.** CAL-33 cells (1.0×10^3 cells/well) were seeded in 12-well plates, then treated and analyzed as described in Materials and Methods. Columns represent the average number of colonies in each treatment group relative to the vehicle-treated group of three biological replicates, and error bars represent standard deviations. Statistical significance was determined as described in Materials and Methods with the experiment-wise type I error rate controlled at 5%. NS = nonsignificant.

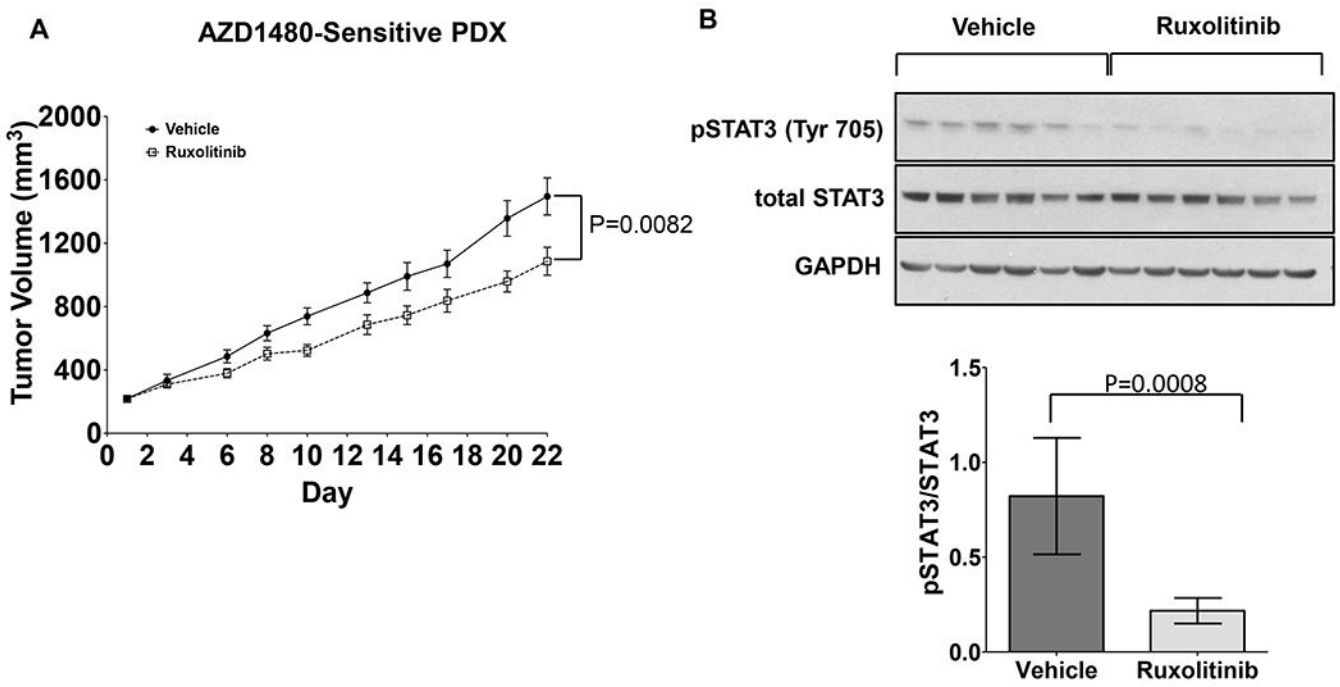

Figure 3. ***In vivo*** **anti-tumor activity of ruxolitinib in HNSCC xenograft model.**

A. A HNSCC PDX previously reported to be inhibited by treatment with the JAK1/2 inhibitor AZD1480 was implanted into both flanks of NSG mice (5 mice and 10 tumors per group). Mouse randomization, treatment, and tumor volume calculations were performed as described in Materials and Methods. Each point on the growth curve represents the average tumor volume on a given day. Error bars represent standard error of the mean. Difference in tumor growth rate between vehicle- and ruxolitinib-treated mice was analyzed by random effects model analysis. **B.** Lysates from tumors in panel A were subjected to immunoblotting for pSTAT3, total STAT3, and GAPDH. Bar graphs represent average pSTAT3 levels quantified with densitometry using ImageJ. Statistical significance was determined as described in Materials and Methods.

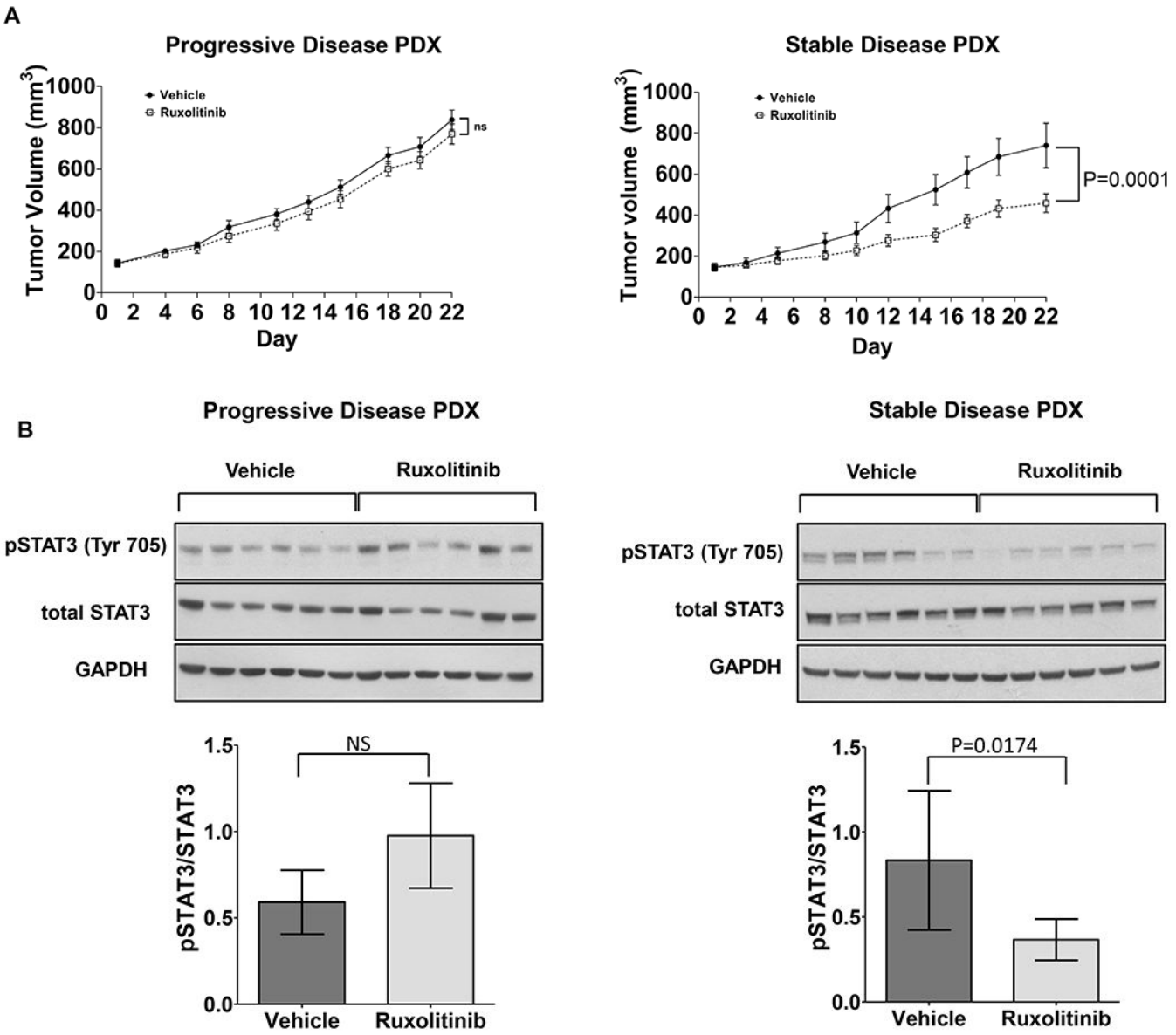

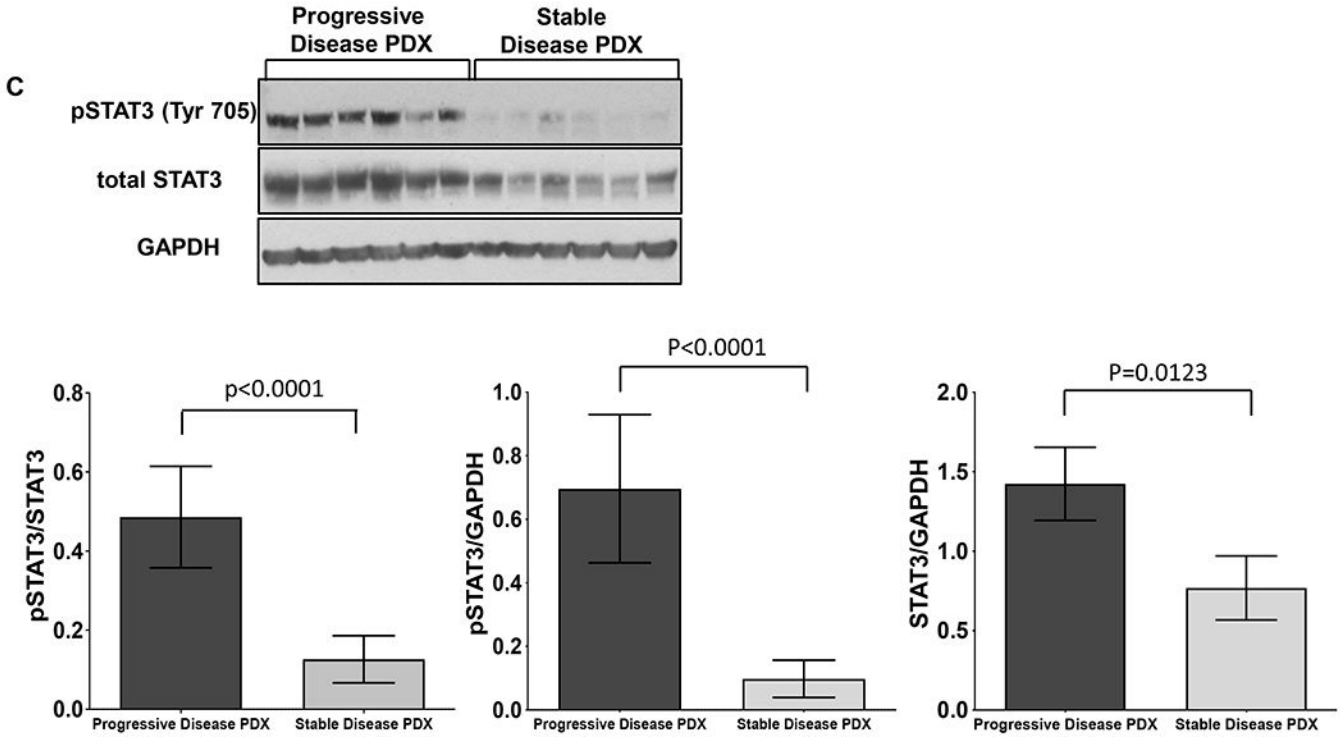

Figure 4. HNSCC PDXs as avatars for clinical response to ruxolitinib.

A. HNSCC tumor samples from patients with progressive disease and stable disease after neoadjuvant ruxolitinib therapy (20 mg twice/day) were implanted into both flanks of NSG mice (5 mice and 10 tumors per group) each. The PDXs were created from tumors resected from patients treated for 15 or 18 days with ruxolitinib (20 mg twice a day) on a window-of-opportunity clinical trial. Mouse randomization, treatment, and tumor volume calculations were performed as described in Materials and Methods. Each point on the growth curve represents the average tumor volume on a given day. Error bars represent standard error of the mean. Differences in tumor growth rate between vehicle- and ruxolitinib-treated mice were analyzed by random effects model analysis (progressive disease PDX $P = 0.7599$; stable disease PDX $P = 0.0001$). **B.** Lysates from vehicle and ruxolitinib-treated PDX tumors were subjected to immunoblotting for pSTAT3, total STAT3, and GAPDH. Columns represent average ratios of pSTAT3/STAT3 as quantified with densitometry using ImageJ. Statistical significance was determined as described in Materials and Methods with the experiment-wise type I error rate controlled at 5%. **C**. Lysates from vehicle- treated PDX tumors were subjected to immunoblotting for pSTAT3, total STAT3, and GAPDH. Columns represent average ratios of pSTAT3/STAT3, pSTAT3/GAPDH, or STAT3/GAPDH as quantified by densitometry using ImageJ. Statistical significance was as described in Materials and Methods with the overall I error rate controlled at 5%.

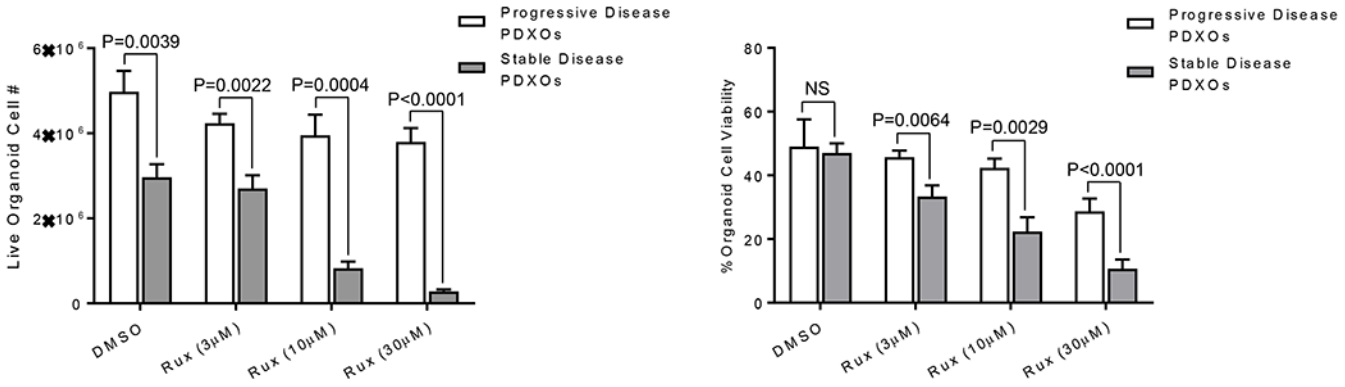

Figure 5.

HNSCC PDXOs as a predictive model for ruxolitinib response. The HNSCC PDX tumors created from patients with progressive disease or stable disease post-ruxolitinib treatment were maintained in immunodeficient NSG mice. Organoids were derived from these PDX tumors (PDXOs), using the air-liquid interface method. Organoid culture, treatment, and viability assays were performed as described in the Materials and Methods. Error bars represent standard deviation of the mean. Differences between progressive disease and stable disease PDXOs were analyzed at each dose of treatment by the unpaired two-samples t-test. Statistical significance was determined with the experiment-wise type I error rate controlled at 5%. NS = nonsignificant.

Table 1

Characteristics of HNSCC Patients

	Progressive Disease Patient	Stable Disease Patient
Age	71	57
Sex	Female	Female
Tumor Site	Oral tongue	Oral tongue
Stage	T2N0M0	T3N1M0
HPV status	p16 negative	Unknown/not done